# REDUCED COMPLEXITY FFT-BASED DOA AND DOD ESTIMATION FOR MOVING TARGET IN BISTATIC MIMO RADAR

*Hussain Ali*[†] *Sajid Ahmed*[⋆] *Tareq Y. Al-Naffouri*[⋆] *Mohamed-Slim Alouini*[⋆]

[†] King Fahd University of Petroleum and Minerals (KFUPM),
Electrical Engineering Department, Dhahran, Saudi Arabia
[⋆] King Abdullah University of Science and Technology (KAUST),
Division of Physical Sciences and Engineering, Thuwal, Saudi Arabia

## ABSTRACT

In this paper, we consider a bistatic multiple-input multiple-output (MIMO) radar. We propose a reduced complexity algorithm to estimate the direction-of-arrival (DOA) and direction-of-departure (DOD) for moving target. We show that the calculation of parameter estimation can be expressed in terms of one-dimensional fast-Fourier-transforms which drastically reduces the complexity of the optimization algorithm. The performance of the proposed algorithm is compared with the two-dimension multiple signal classification (2D-MUSIC) and reduced-dimension MUSIC (RD-MUSIC) algorithms. It is shown by simulations, our proposed algorithm has better estimation performance and lower computational complexity compared to the 2D-MUSIC and RD-MUSIC algorithms. Moreover, simulation results also show that the proposed algorithm achieves the Cramér-Rao lower bound.

***Index Terms***— Bistatic MIMO radar, direction of arrival, direction of departure.

## 1. INTRODUCTION

Multiple-input multiple-output (MIMO) radars have been extensively investigated in literature for surveillance applications. MIMO radar can be seen as an extension of phased array radar, where the transmitted waveforms can be independent or partially correlated. Such waveforms yield extra degrees of freedom that can be exploited for better detection performance and resolution [1], [2], [3], [4]. MIMO radar can be classified as colocated MIMO radar or bistatic MIMO radar based on the location of receiver. Colocated radar has the transmitter and receiver located close to each other. Bistatic MIMO radar has the transmitter and receiver separated by large distances. Bistatic radar has some additional advantages over monostatic radar, e.g. better performance for target detection and covert operation [5]. The target localization in bistatic MIMO radar can be achieved by finding its direction of arrival (DOA) and direction of departure (DOD). The DOA and DOD is the same in colocated MIMO radar whereas in bistatic MIMO radar they are two different unknown parameters. Several algorithms have been proposed in literature for the estimation of these two unknown parameters in bistatic MIMO radars.

The DOA and DOD parameter estimation is a two-dimension search problem for static target. The conventional estimation method of signal parameters via rotational invariance technique (ESPRIT) [6] for DOA and DOD estimation have been presented in [7]. The ESPRIT algorithm exploits the invariance property to convert the two-dimension search problem into two independent one-dimension search problems but it requires pair matching between the estimates of transmit and receive angles. A low complexity ESPRIT algorithm which automatically performs the pair matching is proposed in [8]. Another scheme based on ESPRIT has been proposed in [9] for three transmitters only which is extended and generalized in [10] for any number of transmitters.

The two-dimension multiple signal classification (2D-MUSIC) algorithm has better estimation performance for DOA and DOD estimation than ESPRIT methods but it is computationally expensive because it requires a two-dimension search. In [11], a reduced-complexity multiple signal classification (RD-MUSIC) algorithm has been proposed which requires one-dimension search and its performance is very close to 2D-MUSIC with lesser complexity. A joint DOA and DOD estimation by polynomial root finding technique has been proposed in [12] which is shown to have lesser computational complexity than 2D-MUSIC. Another estimation algorithm based on properties of Kronecker product is discussed in [13] whereas in [14] the DOA and DOD estimation problem for coherent targets has been investigated. In [15], Capon beamformer is used to improve parameter estimation but the presented method requires two-dimension computationally expensive search.

Another method for direction finding in bistatic MIMO radar has been presented in [16] that is based on the solution of a constrained minimization problem to find the directions which is again a computationally expensive method. In [17], the non-circular characteristics of transmitted signals are exploited for DOA and DOA estimation in bistatic MIMO radar. Maximum likelihood estimation for DOA and DOD has been discussed in [18]. In [19], a joint diagonalization based method for DOA and DOD has been proposed. The signal model used in most of the existing work is based on matched filtering with the transmitted signal and assume that the covariance matrix of transmitted signal is identity. The performance of DOA and DOD estimation using velocity sensors are investigated in [20], [21] and reduced complexity algorithms based on MUSIC are derived. The estimation problem for non-uniform array was investigated in [22]. The algorithm proposed in [23] is also based on ESPRIT and MUSIC.

In this work, we derive the estimators for the adaptive Capon beamformer and APES beamformer at the receiver with moving target assumption. This is a three-dimensional search problem. To solve it, we derive a reduced complexity fast-Fourier-transform (FFT)-based algorithm for DOA, DOD and Doppler shift parameter estimation. Unlike existing algorithms, our approach does not de-

This research was funded by a grant from the office of competitive research funding (OCRF) at the King Abdullah University of Science and Technology (KAUST) under grant number URF/1/1713-01-01.

pend on the assumption that the covariance matrix of the transmitted signal is identity. Moreover, the proposed algorithm works without pair matching between the transmit and receive angle estimates.

The paper is organized as follows: The bistatic MIMO radar signal model for DOA and DOD estimation is presented in section 2. Section 3 presents the proposed parameter estimation algorithm for DOA and DOD estimation. Simulation results are presented in section 6 and we conclude the paper in section 7.

**Notation:** Bold lower case letters, $\mathbf{x}$, and bold upper case letters, $\mathbf{X}$, respectively denote vectors and matrices. The notations $\mathbf{X}^{\mathsf{T}}$, $\mathbf{X}^{*}$, $\mathbf{X}^{\mathsf{H}}$ respectively denote the transpose, conjugate of a matrix and conjugate transposition of a matrix $\mathbf{X}$. The operator $\mathrm{E}\{\cdot\}$ denotes statistical expectation. The operator $\mathscr{F}\{\cdot\}$ denotes the fast-Fourier-transform of a vector.

## 2. SIGNAL MODEL

Consider a bistatic MIMO radar setup with $n_T$ antennas at the transmitter and $n_R$ antennas at the receiver. The transmitter and receiver are separated by a large distance. The antenna arrays at the transmitter and receiver are uniform and linear and the inter-element-spacing between any two adjacent antenna elements at the transmitter/receiver is half of the transmitted signal wavelength. Each antenna transmits a narrowband signal using a common carrier frequency. There is a possible point target present at $(\theta_k, \phi_k)$, where $\theta_k$ and $\phi_k$ are respectively the DOD from the transmitter to the target and DOA from the target to the receiver. $\mathbf{s}(n)$ is the vector of transmitted symbols (also known at the receiver) at time index $n$. $\mathbf{y}(n)$ denotes the vector of $n_R$ baseband received samples. $\mathbf{z}(n)$ is the vector of circularly symmetric white Gaussian noise samples at $n_R$ receive antennas. The received signal vector can be written as

$$\mathbf{y}(n) = \beta_k e^{j2\pi n f_{d_k}} \mathbf{a}_R(\phi_k)\mathbf{a}_T^{\mathsf{T}}(\theta_k)\mathbf{s}(n) + \mathbf{z}(n), \quad \text{for } n = 0, 1, \ldots, N-1, \quad (1)$$

where $\beta_k$, $f_{d_k}$, $\mathbf{a}_R(\theta_k) = [1, e^{i\pi\sin(\theta_k)}, \ldots, e^{i\pi(n_R-1)\sin(\theta_k)}]^{\mathsf{T}}$, and $\mathbf{a}_T(\phi_k) = [1, e^{i\pi\sin(\phi_k)}, \ldots, e^{i\pi(n_T-1)\sin(\phi_k)}]^{\mathsf{T}}$ respectively denote reflection coefficient of the target, the Doppler shift of the target, receive steering vector, and transmit steering vector. The total number of snapshots is denoted by $N$. For different range bins, $\theta_k$ and $\phi_k$ will be different. In the following section, we propose a low complexity algorithm to estimate the target parameters.

## 3. PROPOSED ALGORITHM FOR DOA, DOD AND DOPPLER SHIFT ESTIMATION

To increase the signal-to-noise ratio, the received signal vector in (1) can be multiplied by a beamforming weight vector, $\mathbf{w}(\phi_k)$, as

$$\mathbf{w}^{\mathsf{H}}(\phi_k)\mathbf{y}(n) = \beta_k e^{j2\pi n f_{d_k}} \mathbf{w}^{\mathsf{H}}(\phi_k)\mathbf{a}_R(\phi_k)\mathbf{a}_T(\theta_k)^{\mathsf{T}}\mathbf{s}(n) + \mathbf{w}^{\mathsf{H}}(\phi_k)\mathbf{z}(n). \quad (2)$$

There are two approaches to calculate the optimum beamformer which we discuss next.

### 3.1. Capon Beamformer

The beamformer weight vector, which maximizes the signal-to-noise ratio at the receiver can be derived as [24]

$$\mathbf{w}(\phi_k) = \frac{\mathbf{R}_y^{-1}\mathbf{a}_R(\phi_k)}{\mathbf{a}_R^{\mathsf{H}}(\phi_k)\mathbf{R}_y^{-1}\mathbf{a}_R(\phi_k)}, \quad (3)$$

where

$$\mathbf{R}_y = \mathrm{E}\,[\mathbf{y}(n)\mathbf{y}^{\mathsf{H}}(n)] = \frac{\mathbf{Y}\mathbf{Y}^{\mathsf{H}}}{N}.$$

is the covariance matrix of the received signal snapshots. Therefore, to estimate the target parameters using (2) and (3) the cost function to be minimized can be written as

$$\min_{\beta_k,\phi_k,\theta_k,f_{d_k}} \frac{1}{N}\left\|\mathbf{w}^{\mathsf{H}}(\phi_k)\mathbf{Y} - \beta_k\mathbf{a}_T^{\mathsf{T}}(\theta_k)\mathbf{S}\mathbf{F}(f_{d_k})\right\|^2 \quad (4)$$

where $\mathbf{F}(f_{d_k}) = \mathrm{diag}([\ 1 \quad e^{j2\pi f_{d_k}} \quad \ldots \quad e^{j2\pi(N-1)f_{d_k}}\ ])$. (We drop the suffix $(f_{d_k})$ from $\mathbf{F}(f_{d_k})$ in the following for simplicity of notation.) For the minimization of the above cost-function, differentiating with respect to $\beta_k$ and equating the result to zero yields

$$\hat{\beta}_k(\phi_k, \theta_k, f_{d_k}) = \frac{\mathbf{w}^{\mathsf{H}}(\phi_k)\mathbf{Y}\mathbf{F}^{\mathsf{H}}\mathbf{S}^{\mathsf{H}}\mathbf{a}_T^{*}(\theta_k)}{N\mathbf{a}_T^{\mathsf{T}}(\theta_k)\mathbf{R}_s\mathbf{a}_T^{*}(\theta_k)}. \quad (5)$$

where

$$\mathbf{R}_s = \mathrm{E}\,[\mathbf{s}(n)\mathbf{s}^{\mathsf{H}}(n)] = \frac{\mathbf{S}\mathbf{S}^{\mathsf{H}}}{N}$$

is the covariance matrix of transmitted signal. Since $\hat{\beta}_k$ is a function of $\phi_k$, $\theta_k$ and $f_{d_k}$, to estimate these parameters we subsitute (5) in (4) and use (3) to get the following cost function

$$J_1(\phi_k, \theta_k, f_{d_k}) = \mathbf{w}^{\mathsf{H}}(\phi_k)\mathbf{R}_y\mathbf{w}(\phi_k) - \frac{\left|\mathbf{w}^{\mathsf{H}}(\phi_k)\mathbf{Y}\mathbf{F}^{\mathsf{H}}\mathbf{S}^{\mathsf{H}}\mathbf{a}_T^{*}(\theta_k)\right|^2}{N^2\mathbf{a}_T^{\mathsf{T}}(\theta_k)\mathbf{R}_s\mathbf{a}_T^{*}(\theta_k)} \quad (6)$$

$$= \frac{1}{\mathbf{a}_R^{\mathsf{H}}(\phi_k)\mathbf{R}_y^{-1}\mathbf{a}_R(\phi_k)} - \frac{|\mathbf{a}_R^{\mathsf{H}}(\phi_k)\mathbf{R}_y^{-1}\mathbf{X}\mathbf{a}_T^{*}(\theta_k)|^2}{N^2[\mathbf{a}_T^{\mathsf{T}}(\theta_k)\mathbf{R}_s\mathbf{a}_T^{*}(\theta_k)][\mathbf{a}_R^{\mathsf{H}}(\phi_k)\mathbf{R}_y^{-1}\mathbf{a}_R(\phi_k)]^2} \quad (7)$$

where we define $\mathbf{X} = \mathbf{Y}\mathbf{F}^{\mathsf{H}}\mathbf{S}^{\mathsf{H}}$ in (7). The minimization of the cost function $J_1(\phi_k, \theta_k, f_{d_k})$ in (7) gives us the estimates $\hat{\phi}_k, \hat{\theta}_k, \hat{f}_{d_k}$ of unknown parameters.

### 3.2. APES Beamformer

Next, we derive the cost function using APES beamformer at the receiver by following [25]. The cost function $J_1(\phi_k, \theta_k, f_{d_k})$ in (6) can be written as

$$J_2(\phi_k, \theta_k, f_{d_k}) = \min_{\mathbf{w}} \mathbf{w}^{\mathsf{H}}\mathbf{Q}\mathbf{w}, \quad \text{subject to } \mathbf{w}^{\mathsf{H}}(\phi_k)\mathbf{a}_r(\phi_k) = 1 \quad (8)$$

which yields

$$\mathbf{w}(\phi) = \frac{\mathbf{Q}^{-1}\mathbf{a}_R(\phi_k)}{\mathbf{a}_R^{\mathsf{H}}(\phi_k)\mathbf{Q}^{-1}\mathbf{a}_R(\phi_k)} \quad (9)$$

where

$$\mathbf{Q} = \mathbf{R}_y - \frac{\mathbf{X}\mathbf{a}_T^{*}(\theta_k)\mathbf{a}_T^{\mathsf{T}}(\theta_k)\mathbf{X}^{\mathsf{H}}}{N^2\mathbf{a}_T^{\mathsf{T}}(\theta_k)\mathbf{R}_s\mathbf{a}_T^{*}(\theta_k)} \quad (10)$$

Using (9) to solve (8),

$$\begin{aligned} J_2(\phi_k, \theta_k, f_{d_k}) &= \min_{\phi_k,\theta_k,f_{d_k}} \frac{1}{\mathbf{a}_R^{\mathsf{H}}(\phi_k)\mathbf{Q}^{-1}\mathbf{a}_R(\phi_k)} \\ &= \max_{\phi_k,\theta_k,f_{d_k}} \mathbf{a}_R^{\mathsf{H}}(\phi_k)\mathbf{Q}^{-1}\mathbf{a}_R(\phi_k) \\ &= \max_{\phi_k,\theta_k,f_{d_k}} \mathbf{a}_R^{\mathsf{H}}(\phi_k)\mathbf{R}_y^{-1}\mathbf{a}_R(\phi_k) + \\ &\quad \frac{|\mathbf{a}_R^{\mathsf{H}}(\phi_k)\mathbf{R}_y^{-1}\mathbf{X}\mathbf{a}_T^{*}(\theta_k)|^2}{N^2\mathbf{a}_T^{\mathsf{T}}(\theta_k)\mathbf{R}_s\mathbf{a}_T^{*}(\theta_k) - \mathbf{a}_T^{\mathsf{T}}(\theta_k)\mathbf{X}^{\mathsf{H}}\mathbf{R}_y^{-1}\mathbf{X}\mathbf{a}_T^{*}(\theta_k)} \end{aligned} \quad (11)$$

where we have used the Sherman-Morrison formula to find the inverse of $\mathbf{Q}$. The maximization of $J_2(\phi_k, \theta_k, f_{d_k})$ in (11) gives us the estimates $\hat{\phi}_k, \hat{\theta}_k, \hat{f}_{d_k}$ of the unknown parameters.

## 4. REDUCED COMPLEXITY FFT-BASED SOLUTION

The evaluation of (7) and (11) requires a three-dimensional search. The terms that need to be evaluated in (7) are $\mathbf{a}_R^{\mathsf{H}}(\phi_k)\mathbf{R}_y^{-1}\mathbf{a}_R(\phi_k)$, $\mathbf{a}_T^{\mathsf{T}}(\theta_k)\mathbf{R}_s\mathbf{a}_T^{*}(\theta_k)$ and $\mathbf{a}_R^{\mathsf{H}}(\phi_k)\mathbf{R}_y^{-1}\mathbf{X}\mathbf{a}_T^{*}(\theta_k)$. The equation (11) also requires the evaluation of the same three terms as in (7) with an additional fourth term $\mathbf{a}_T^{\mathsf{T}}(\theta_k)\mathbf{X}^{\mathsf{H}}\mathbf{R}_y^{-1}\mathbf{X}\mathbf{a}_T^{*}(\theta_k)$. The solution of (7) and (11) in three-dimension gives us the estimate of unknown parameters. The computational load is on the term $\mathbf{a}_R^{\mathsf{H}}(\phi_k)\mathbf{R}_y^{-1}\mathbf{X}\mathbf{a}_T^{*}(\theta_k)$ which is to be evaluated in three-dimensions. In the following, we show that how this term can be expressed as FFTs and we evaluate it step-by-step for each of the three dimensions.

*Step 1:* Let's vectorize $\mathbf{X}$ as follows

$$\text{vec}(\mathbf{X}) = \text{vec}(\mathbf{Y}\mathbf{F}^{\mathsf{H}}\mathbf{S}^{\mathsf{H}}) \tag{12}$$

$$\text{vec}(\mathbf{X}) = [\mathbf{S}^{*} \otimes \mathbf{Y}]\text{vec}(\mathbf{F}^{\mathsf{H}}) \tag{13}$$

$$\text{vec}(\mathbf{X}) = [\mathbf{K}_{sy}]_{(n_T n_R \times N^2)}\, \text{vec}(\mathbf{F}^{\mathsf{H}}) \tag{14}$$

where we have defined $\mathbf{K}_{sy} = \mathbf{S}^{*} \otimes \mathbf{Y}$. Since $\mathbf{F}^{\mathsf{H}}$ is a diagonal matrix, $\text{vec}(\mathbf{F}^{\mathsf{H}})$ has at most $N$ non-zero values. Therefore, by choosing non-zero entries in $\text{vec}(\mathbf{F}^{\mathsf{H}})$ and corresponding columns in $\mathbf{K}_{sy}$, we can write the equivalent of (14) as

$$\text{vec}(\mathbf{X}) = \left[\mathbf{K}'_{sy}\right]_{(n_T n_R \times N)} \mathbf{a}(f_k) \tag{15}$$

where $\mathbf{a}(f_k) = [\ 1 \quad e^{-j2\pi f_{d_k}} \quad \ldots \quad e^{-j2\pi(N-1)f_{d_k}}\ ]^{\mathsf{T}}$. Now for any row vector $\mathbf{k}^{\mathsf{T}}$ in $\mathbf{K}'_{sy}$,

$$\mathbf{k}^{\mathsf{T}}\mathbf{a}(f_k) = \sum_{n=0}^{N-1} k_n e^{-j2\pi n f_k} \tag{16}$$

This is equivalent to evaluating the FFT of $\mathbf{k}_l^{\mathsf{T}}$, $\mathscr{F}[\mathbf{k}_l^{\mathsf{T}}]$. Thus (15) can be evaluated for all $f_k \in [-\frac{1}{2}, -\frac{1}{2}]$ for a given resolution by taking row-by-row $N_{FFT}$-point FFT of $\mathbf{K}'_{sy}$. After evaluating $\mathscr{F}[\mathbf{K}'_{sy}]$, we get back $[\mathbf{X}]_{(n_R \times n_T)}$ by reshaping $[\text{vec}(\mathbf{X})]_{(n_T n_R \times 1)}$.

*Step 2:* The next step is to evaluate $\mathbf{X}\mathbf{a}_T^{*}(\theta_k)$ which is the solution for the second dimension $\theta_k$. It can be easily shown in a similar way to (16) that for any row vector $\mathbf{x}^{\mathsf{T}}$ in $\mathbf{X}$, we have

$$\begin{aligned}\mathbf{x}^{\mathsf{T}}\mathbf{a}_T^{*}(\theta_k) &= \sum_{p=0}^{n_T-1} x_p e^{-j\pi p \sin(\theta_k)} \\ &= \sum_{p=0}^{n_T-1} x_p e^{-j2\pi p f_{\theta_k}} \equiv \mathscr{F}[\mathbf{x}^{\mathsf{T}}]\end{aligned} \tag{17}$$

where $f_{\theta_k} = \frac{\sin(\theta_k)}{2} \in [-\frac{1}{2}, \frac{1}{2}]$.

*Step 3:* The third step is to evaluate $\mathbf{a}_R^{\mathsf{H}}(\phi_k)\mathbf{R}_y^{-1}$ which is the third dimension $\phi_k$. For any column vector $\mathbf{r}$ in $\mathbf{R}_y^{-1}$, we have

$$\begin{aligned}\mathbf{a}_R^{\mathsf{H}}(\phi_k)\mathbf{r} &= \sum_{m=0}^{n_R-1} r_m e^{-j\pi m \sin(\phi_k)} \\ &= \sum_{m=0}^{n_R-1} r_m e^{-j2\pi m f_{\phi_k}} \equiv \mathscr{F}[\mathbf{r}]\end{aligned} \tag{18}$$

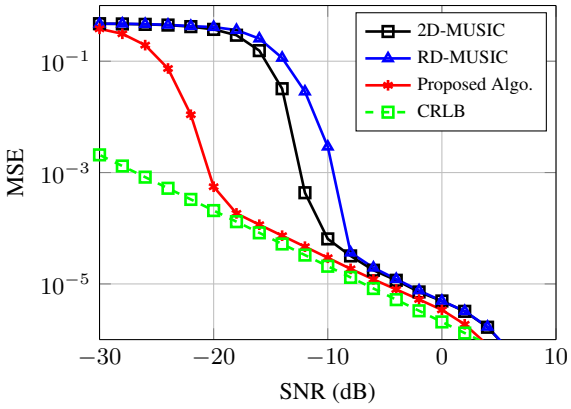


**Fig. 1**. MSE performance for DOA estimation ($\hat{\phi}_k$) using $J_1(\phi_k, \theta_k)$. Simulation parameters: $N = 256$, $n_T = 10$, $n_R = 10$.

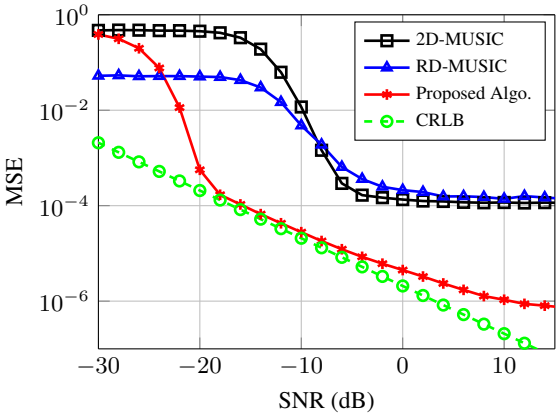


**Fig. 2**. MSE performance for DOD estimation ($\hat{\theta}_k$) using $J_1(\phi_k, \theta_k)$. Simulation parameters: $N = 256$, $n_T = 10$, $n_R = 10$.

where $f_{\phi_k} = \frac{\sin(\phi_k)}{2} \in [-\frac{1}{2}, \frac{1}{2}]$.

The three-dimensional term $\mathbf{a}_R^{\mathsf{H}}(\phi_k)\mathbf{R}_y^{-1}\mathbf{X}\mathbf{a}_T^{*}(\theta_k)$ can be solved by using above-mentioned three steps. The terms $\mathbf{a}_R^{\mathsf{H}}(\phi_k)\mathbf{R}_y^{-1}\mathbf{a}_R(\phi_k)$ and $\mathbf{a}_T^{\mathsf{T}}(\theta_k)\mathbf{R}_s\mathbf{a}_T^{*}(\theta_k)$ are one-dimensional, so there evaluation is straight forward. The term $\mathbf{a}_T^{\mathsf{T}}(\theta_k)\mathbf{X}^{\mathsf{H}}\mathbf{R}_y^{-1}\mathbf{X}\mathbf{a}_T^{*}(\theta_k)$ is a two-dimensional term and it can be evaluated in a similar way by FFTs as discussed above. Therefore, the cost function in (7) and (11) can be solved efficiently by the above mentioned procedure using FFT for grid of size $N_{FFT}$-points. The minimum and maximum of the solution of (7) and (11) respectively gives us the estimates of unknown parameters $\hat{f}_{\theta_k}$, $\hat{f}_{\phi_k}$ and $\hat{f}_{d_k}$. We can find $\hat{\theta}_k$ and $\hat{\phi}_k$ by using the relations $\hat{\theta}_k = \sin^{-1}(2\hat{f}_{\theta_k})$ and $\hat{\phi}_k = \sin^{-1}(2\hat{f}_{\phi_k})$.

Static target case is a special case of the above formulation when the Doppler shift is zero and $\mathbf{F}$ vanishes. We solve the static target case for comparison with 2D-MUSIC and RD-MUSIC.

## 5. COMPLEXITY ANALYSIS

We discuss the complexity of our proposed algorithm in comparison with 2D-MUSIC and RD-MUSIC algorithms for static target case. The 2D-MUSIC algorithm requires $\boldsymbol{O}\{Nn_T^2n_R^2 + n_T^3n_R^3 + m^2[n_Tn_R(n_Tn_R - K) + n_Tn_R - K]\}$ for $m$ searches and $K$ targets.

(Note that $m$ represents number of grid points which is represented by $N_{FFT}$ for our algorithm.) The second algorithm used for comparison is RD-MUSIC which requires be $\boldsymbol{O}\{N^2n_T^2n_R^2 + n_T^3n_R^3 + m[n_T^2n_R(n_Tn_R-K)+n_T^2(n_Tn_R-K)+n_T^2]\}$ where the complexity reduction is achieved by reducing $m^2$ factor to $m$ by converting the 2D-search problem into two one-dimensional searches. Our Proposed algorithm requires $\boldsymbol{O}\{n_R^2N + n_R^2 + n_R[N_{FFT}\log N_{FFT}] + n_RNn_T + n_R[N_{FFT}\log N_{FFT}] + N_{FFT}^2n_R + N_{FFT}[n_TN+N] + N_{FFT}n_R\}$. The complexity of our proposed algorithm is lower than both 2D-MUSIC and RD-MUSIC algorithms because our algorithm exploits low complexity of FFT. The average runtime for the three above mentioned algorithms is independent of signal to noise ratio. The average runtime per iteration was found to be 42.5, 0.17 and 0.05 seconds for 2D-MUSIC, RD-MUSIC and our proposed algorithm respectively.

## 6. SIMULATION RESULTS

We run some simulations to validate the algorithm proposed in this work. We assume that a single target lies on the grid at $(\theta_k, \phi_k)$. The three parameters to be estimated ($\theta_k$ and $\phi_k$) are generated randomly according to $[\theta_k, \phi_k] \sim \mathcal{U}(-10^\circ, 10^\circ)$ and the normalized Doppler shift $f_{d_k} \sim \mathcal{U}(-0.25, 0.25)$. $\beta_k$ is also generated randomly according to $\beta_k \sim e^{i\varphi}$ where $\varphi \sim \mathcal{U}(0, 1)$. The grid search is varied from $-90^\circ$ to $+90^\circ$. The transmitted signals are uncorrelated quadrature phase shift keying (QPSK) symbols. The noise is assumed to be uncorrelated Gaussian with zero mean and variance $\sigma^2$. The noise variance $\sigma^2$ was varied to control the signal-to-noise ratio (SNR). For the simulations, SNR is defined as SNR $= 10\log(1/\sigma^2)$ where the power at each antenna is normalized so that total transmit power is unity.

In Fig. 1 and Fig. 2, we plot the mean-square-error (MSE) error performance for the DOA ($\hat{\phi}_k$) estimation and DOD ($\hat{\theta}_k$) estimation respectively, of the proposed algorithm for static target case. We also compare the performance of our algorithm with both 2D-MUSIC and RD-MUSIC algorithms. We also plot the Cramér-Rao lower bound (CRLB) which is found by inverting the Fisher information matrix obtained using Slepian-Bang's formula (CRLB derivation is not shown here due to space limitation). The number of antenna elements are $n_T = 10$ and $n_R = 10$, the number of snapshots $N$ are 256 and the number of grid points are 512. The 2D-MUSIC and RD-MUSIC algorithms have almost the same performance. The results show that our proposed algorithm outperforms 2D-MUSIC and RD-MUSIC algorithms. Moreover, the performance of proposed algorithm achieves the CRLB. The error floor that appears in the MSE of $\hat{\theta}_k$ for 2D-MUSIC and RD-MUSIC requires some explanation. The signal model used in 2D-MUSIC and RD-MUSIC assumes that the transmitted signals are fully uncorrelated and orthogonal, i.e. $\mathrm{E}\,[\mathbf{s}(n)\mathbf{s}^{\mathsf{H}}(n)] = \mathbf{I}$ where $\mathbf{I}$ is the identity matrix. If the transmitted signals are not fully uncorrelated, then 2D-MUSIC and RD-MUSIC algorithms fail to recover $\theta_k$. Our approach utilizes $\mathbf{s}(n)$ and does not require the assumption $\mathrm{E}\,[\mathbf{s}(n)\mathbf{s}^{\mathsf{H}}(n)] = \mathbf{I}$, therefore, it outperforms both 2D-MUSIC and RD-MUSIC algorithms in estimating $\theta_k$.

Next we show the MSE performance of the unknown parameters for the moving target case. In Fig. 3, we show the MSE performance of by the estimating the three unknown parameters $\hat{\theta}_k, \hat{\phi}_k, \hat{f}_{d_k}$ together. Minimizing cost function $J_1(\phi_k, \theta_k, f_{d_k})$, the Doppler estimation gives good results. Similarly, we plot MSE for the unknown parameters using the cost function $J_2(\phi_k, \theta_k, f_{d_k})$ in Fig. 4. The estimator of $J_2(\phi_k, \theta_k, f_{d_k})$ has slightly improved estimation of $\theta_k$ as

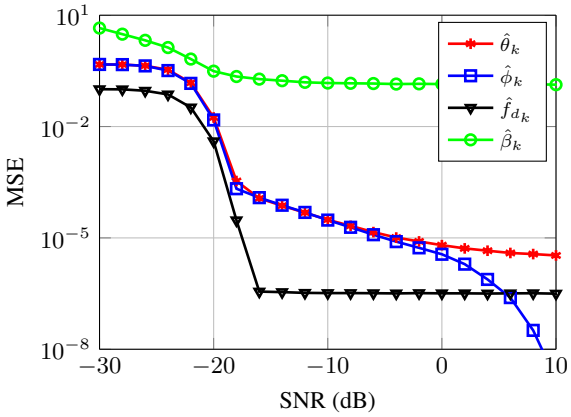


**Fig. 3**. MSE performance for $\hat{\theta}_k$, $\hat{\phi}_k$, $\hat{\beta}_k$ and $\hat{f}_{d_k}$ using $J_1(\phi_k, \theta_k, f_{d_k})$. Simulation parameters: $N = 256$, $n_T = 10$, $n_R = 10$.

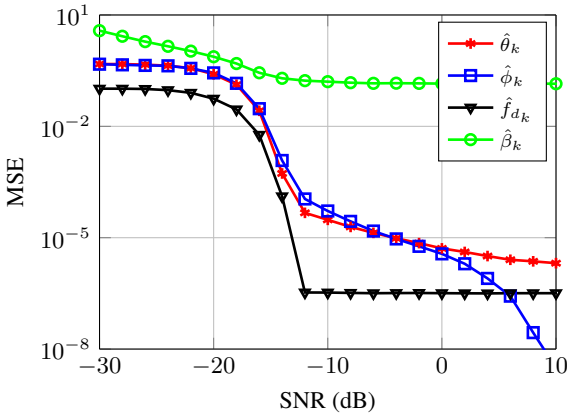


**Fig. 4**. MSE performance for $\hat{\theta}_k$, $\hat{\phi}_k$, $\hat{\beta}_k$ and $\hat{f}_{d_k}$ using $J_2(\phi_k, \theta_k, f_{d_k})$. Simulation parameters: $N = 256$, $n_T = 10$, $n_R = 10$.

compared to the estimator of $J_1(\phi_k, \theta_k, f_{d_k})$. However, the Doppler estimation using cost function $J_1(\phi_k, \theta_k, f_{d_k})$ is better as compared to cost function $J_2(\phi_k, \theta_k, f_{d_k})$. The error floor in MSE of $\hat{f}_{d_k}$ appears because estimation of $f_{d_k}$ is done on a finite grid. It can also be noted that the $J_2(\phi_k, \theta_k, f_{d_k})$ estimation has better $\hat{\beta}_k$ estimation than $J_1(\phi_k, \theta_k, f_{d_k})$ due to the fact that $\hat{\beta}_k$ estimates obtained by $J_1(\phi_k, \theta_k, f_{d_k})$ are always biased.

## 7. CONCLUSION

In this paper, we present a new FFT-based DOA, DOD and Doppler shift estimation algorithm using two adaptive beamformer at the receiver for bistatic MIMO radar. We derive the cost functions for both Capon and APES estimators for the moving target case. We show that the proposed FFT-based algorithm has the best performance with lowest complexity. The algorithm also utilizes the transmitted waveform in the parameter estimation and also there is no need of additional algorithm for pair matching. Since, FFT can be deployed easily on hardware, therefore, the approach presented here is also practical in radar applications.

## 8. REFERENCES


[1] J. Li and P. Stoica, "MIMO Radar with Colocated Antennas," *IEEE Signal Processing Magazine*, vol. 24, no. 5, pp. 106–114, sep 2007.

[2] S. Ahmed, J. S. Thompson, Y. R. Petillot, and B. Mulgrew, "Finite Alphabet Constant-Envelope Waveform Design for MIMO Radar," *IEEE Transactions on Signal Processing*, vol. 59, no. 11, pp. 5326–5337, nov 2011.

[3] S. Ahmed, J. S. Thompson, Y. R. Petillot, and B. Mulgrew, "Unconstrained synthesis of covariance matrix for MIMO radar transmit beampattern," *IEEE Transactions on Signal Processing*, vol. 59, no. 8, pp. 3837–3849, 2011.

[4] J. Lipor, S. Ahmed, and M. S. Alouini, "Fourier-Based Transmit Beampattern Design Using MIMO Radar," *IEEE Transactions on Signal Processing*, vol. 62, no. 9, pp. 2226–2235, may 2014.

[5] A. Haimovich, R. Blum, and L. Cimini, "MIMO Radar with Widely Separated Antennas," *IEEE Signal Processing Magazine*, vol. 25, no. 1, pp. 116–129, 2008.

[6] R. Roy and T. Kailath, "ESPRIT-estimation of signal parameters via rotational invariance techniques," *IEEE Transactions on Acoustics, Speech, and Signal Processing*, vol. 37, no. 7, pp. 984–995, jul 1989.

[7] C. Duofang, C. Baixiao, and Q. Guodong, "Angle estimation using ESPRIT in MIMO radar," *Electronics Letters*, vol. 44, no. 12, pp. 770, 2008.

[8] C. Jinli, G. Hong, and S. Weimin, "Angle estimation using ESPRIT without pairing in MIMO radar," *Electronics Letters*, vol. 44, no. 24, pp. 1422–1423, 2008.

[9] M. Jin, G. Liao, and J. Li, "Joint DOD and DOA estimation for bistatic MIMO radar," *Signal Processing*, vol. 89, no. 2, pp. 244–251, feb 2009.

[10] J. Chen, H. Gu, and W. Su, "A new method for joint DOD and DOA estimation in bistatic MIMO radar," *Signal Processing*, vol. 90, no. 2, pp. 714–718, feb 2010.

[11] X. Zhang, L. Xu, and D. Xu, "Direction of Departure (DOD) and Direction of Arrival (DOA) Estimation in MIMO Radar with Reduced-Dimension MUSIC," *IEEE Communications Letters*, vol. 14, no. 12, pp. 1161–1163, dec 2010.

[12] M. L. Bencheikh, Y. Wang, and H. He, "Polynomial root finding technique for joint DOA DOD estimation in bistatic MIMO radar," *Signal Processing*, vol. 90, no. 9, pp. 2723–2730, sep 2010.

[13] X. Liu and G. Liao, "Reduced-dimensional angle estimation in bistatic MIMO radar system," in *Proceedings of IEEE CIE International Conference on Radar*, oct 2011, pp. 67–70.

[14] J. Wang, "Angle estimation of coherent targets for bistatic MIMO radar," in *Proceedings of IEEE CIE International Conference on Radar*, oct 2011, number 2, pp. 989–992.

[15] H. Yan, J. Li, and G. Liao, "Multitarget Identification and Localization Using Bistatic MIMO Radar Systems," *EURASIP Journal on Advances in Signal Processing*, vol. 2008, no. ID 283483, 2008.

[16] R. Xie, Z. Liu, and J.-x. Wu, "Direction finding with automatic pairing for bistatic MIMO radar," *Signal Processing*, vol. 92, no. 1, pp. 198–203, jan 2012.

[17] W. Wang, X. Wang, and X. Li, "Propagator method for angle estimation of non-circular sources in bistatic MIMO radar," in *IEEE Radar Conference*, apr 2013, pp. 1–5.

[18] B. Tang, J. Tang, Y. Zhang, and Z. Zheng, "Maximum likelihood estimation of DOD and DOA for bistatic MIMO radar," *Signal Processing*, vol. 93, no. 5, pp. 1349–1357, may 2013.

[19] T. Q. Xia, "Joint diagonalization based DOD and DOA estimation for bistatic MIMO radar," *Signal Processing*, vol. 108, pp. 159–166, mar 2015.

[20] J. Li and X. Zhang, "Improved Joint DOD and DOA Estimation for MIMO Array With Velocity Receive Sensors," *IEEE Signal Processing Letters*, vol. 18, no. 12, pp. 717–720, dec 2011.

[21] J. He, M. N. S. Swamy, and M. O. Ahmad, "Joint DOD and DOA Estimation for MIMO Array With Velocity Receive Sensors," *IEEE Signal Processing Letters*, vol. 18, no. 7, pp. 399–402, jul 2011.

[22] B. Yao, W. Wang, and Q. Yin, "DOD and DOA Estimation in Bistatic Non-Uniform Multiple-Input Multiple-Output Radar Systems," *IEEE Communications Letters*, vol. 16, no. 11, pp. 1796–1799, nov 2012.

[23] W. Shi, J. Huang, C. He, and J. Han, "Joint Direction-Of-Departure and Direction-Of-Arrival estimation in MIMO array," in *IEEE International Conference of IEEE Region 10 (TENCON 2013)*, oct 2013, pp. 1–4.

[24] J. Capon, "High-resolution frequency-wavenumber spectrum analysis," *Proceedings of the IEEE*, vol. 57, no. 8, pp. 1408–1418, 1969.

[25] P. Stoica, "A new derivation of the APES filter," *IEEE Signal Processing Letters*, vol. 6, no. 8, pp. 205–206, aug 1999.